Transport Studies in HSX at 1 Tesla

J. Lore, F.S.B Anderson, J.M. Canik, W. Guttenfelder, K.M. Likin, J.N. Talmadge, K.Zhai

HSX Plasma Laboratory, University of Wisconsin

Initial results at B=1.0T at HSX demonstrate a reduction in particle and heat transport due to quasisymmetry, supporting the results of B=0.5T operations. Electron temperature and density profiles from Thomson scattering for several injected powers show a factor of 2-2.5 increase in the core temperature and a more peaked density profile for the quasi-helically symmetric configuration (QHS) as compared to the configuration where the symmetry is spoiled (Mirror). In a case where the temperature profiles are matched (requiring 2.3 times the injected power in Mirror) the core electron thermal diffusivity has been measured to be reduced by a factor of 3. The particle transport was analyzed using the neutral gas transport code DEGAS to obtain the source rate. These results indicate that for a given temperature gradient the particle flux, which is dominated by thermodiffusion, is smaller in QHS. Additional work is required on neoclassical calculations before conclusions on the effect of quasisymmetry on anomalous transport can be made.

Keywords: Neoclassical transport, quasisymmetry, DKES, DEGAS, HSX, Thermal transport

1. Introduction

The Helically Symmetric Experiment (HSX) is a mid-sized stellarator at the University of Wisconsin. The magnetic field of HSX can be varied from a quasi-helically symmetric configuration (QHS) to a configuration with the symmetry intentionally degraded by a set of toroidal field coils (Mirror). Aside from the magnetic spectrum, other properties such as the rotational transform, plasma volume and well depth are very similar. The change in the magnetic spectrum can be quantified by the effective ripple, which is increased in the core from 0.007 in QHS to 0.05 in Mirror with the largest change occurring in the core of the plasma. In this paper the effect of spoiling the symmetry on particle and electron heat transport will be discussed.

2. 0.5 Tesla Operation

A transport analysis at B=0.5T demonstrated that both the particle and electron heat transport were reduced in the QHS configuration [1]. For the same injected power the density profiles were peaked in QHS and hollow in Mirror due to a reduction in the thermodiffusive particle flux. It was also shown that 2.3 times the injected power is required in Mirror to match the temperature profiles between the configurations, and that for this matched case the electron thermal diffusivity is reduced in the core for the QHS configuration. The reduction in the core diffusivity was comparable to the calculated difference in the neoclassical diffusivities.

The transport analysis at B=0.5T was complicated by the presence of a suprathermal electron population driven by the 2nd harmonic X-Mode electron cyclotron heating. This suprathermal tail was observed by measurements from several diagnostics including the ECE system, hard X-ray detectors and a diamagnetic loop. Due to the contamination of the diamagnetic loop signal, the absorbed power was measured using many discharges while varying the Thomson scattering firing time around the ECH turnoff time. This limitation meant that very few configurations could be studied at B=0.5T.

3. 1.0 Tesla Operation

HSX has recently began regular operation at B=1.0T. At the higher field strength fundamental frequency O-Mode heating is used greatly reducing the drive of a suprathernal population. Fundamental frequency heating also allows for operation at higher densities, increasing the damping on a tail population. Measurements from the ECE system and the diamagnetic loop indicate that the suprathermal contamination has been greatly suppressed at B=1.0T allowing for a transport analysis to be performed at several injected powers in both QHS and Mirror.

4. Profiles from Thomson Scattering

A ten channel Thomson scattering system installed on HSX has been used to measure the electron density and temperature profiles in the QHS and Mirror configurations for four injected powers: 26, 44, 70 and 100kW.

The profiles shown in Figure 1 clearly show that for each injected power the central electron temperatures are 2-2.5 times greater in the QHS configuration. Also, for each injected power above 26kW the density profiles are more peaked for QHS. The greatest differences in the profiles are seen in the core, where the change in effective ripple is the largest and neoclassical transport is significant (see Section 7). These profiles indicate that transport properties change between the two configurations and that

author's e-mail: jlore@wisc.edu

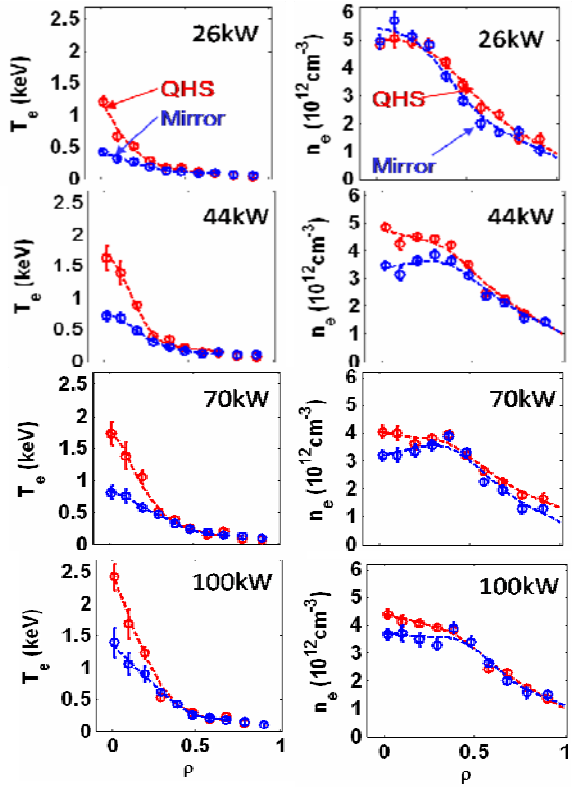

Fig.1 QHS and Mirror electron temperature (left) and density (right) profiles for several injected powers.

both particle and electron thermal transport are improved in the QHS configuration.

Due to the differences in the temperature gradients, the profiles cannot be exactly matched between the configurations. To minimize the difference in the profiles over the whole minor radius 2.3 times the injected power (1.8 times the absorbed power) is needed in the Mirror configuration, again demonstrating the improvement in electron thermal transport (Figure 2).

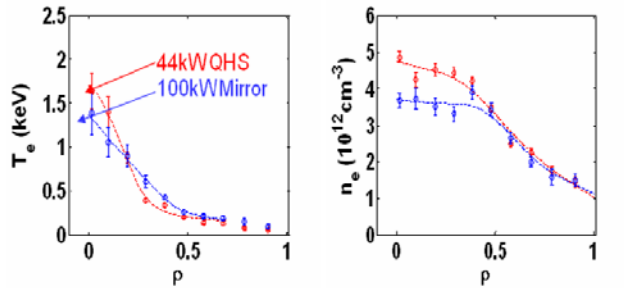

Fig.2 Profiles demonstrating that 2.3 times the injected power is required in Mirror to minimize the difference in the temperature profiles.

5. Electron Thermal Transport

To quantify the change in thermal transport seen in Figure 2 the electron thermal diffusivities were calculated. An expression for the diffusivity can be obtained by taking the flux surface average of the energy continuity equation (1).

$$\frac{d}{dt}\left(\frac{3}{2}n_e T_e\right) = -\nabla\cdot\mathbf{q} + p_{in} - p_{out} \qquad (1)$$

Where p_{in} and p_{out} are generic power sources and sinks. Assuming that the heat flux is purely diffusive, the effective electron thermal diffusivity can be written as seen in (2).

$$\chi_e = \frac{-\int_0^{\rho} V'(p_{in} - p_{out})d\rho'}{n_e\left\langle V'\frac{\partial T_e}{\partial\rho}|\nabla\rho|^2\right\rangle} \qquad (2)$$

Where $V'=dV/d\rho$ and $\nabla\rho$ account for the deviation of the geometry from a straight cylinder.

For the following calculations the power sinks such as radiation and ionization losses were ignored. These losses are small compared to the total injected power for HSX plasmas and were found to be similar between the configurations at B=0.5T [2].

A ray-tracing code is used to calculate the power deposition profiles based on the local temperature and density from the Thomson scattering profiles. The power deposition profiles are volume integrated and scaled to match the absorbed power calculated at ECH turnoff from the diamagnetic loop.

Figure 3 shows the effective thermal diffusivities for the profiles in Figure 2. The diffusivity in the core has been reduced by a factor of three due to quasi-symmetry.

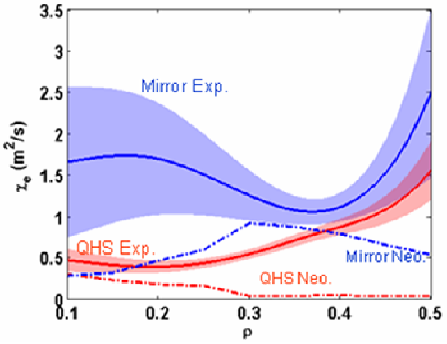

Fig.3 Experimental and neoclassical effective thermal diffusivities for the QHS and Mirror profiles in Figure 2.

6. Particle Transport

The density profiles seen in Figure 1 indicate that the particle transport changes in the core of the plasma between the two configurations. At B=0.5T it was found that the thermodiffusive component of the particle flux was reduced in the QHS configuration. At B=1.0T

neoclassical calculations show that the thermodiffusive component is the dominant particle flux drive in both configurations (Figure 4).

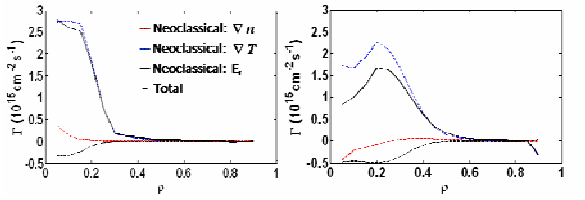

Fig.4 Components of the neoclassical particle flux for QHS (left) and Mirror (right). In each configuration the dominant component is thermodiffusion.

To calculate the experimental particle flux the particle source rate is required. To obtain the source rate the neutral transport code DEGAS was used [3]. DEGAS is a 3D Monte Carlo code that can calculate several quantities including, significantly, the H_α emission. The code is run for each set of Thomson scattering profiles on a fully 3D computational grid representing the HSX vacuum vessel. The results of the code are coupled to experiment using a suite of absolutely calibrated H_α detectors located on the machine.

For each set of profiles DEGAS is run for two cases. One of the cases is for the main fuelling source, a puff valve located on the vessel wall. DEGAS calculates the H_α emission to be localized toroidally for this case, and the results are then scaled to match the measured H_α emission from a poloidal array located at the puff valve. The other case is for a recycling source, located at the locations where the magnetic field lines just outside the separatrix intersect the vessel. The results from this case are scaled to match the measured emission from a toroidal array of detectors. The scaled results of the two cases are then added to obtain the total source rate.

The particle flux can be calculated by taking the flux surface average of the particle continuity equation (3) ins steady state yielding (4).

$$\frac{\partial n}{\partial t} + \nabla \cdot \Gamma = S \tag{3}$$

$$\Gamma = \frac{1}{\langle \nabla \rho \rangle V'} \int_0^\rho V' S(\rho') d\rho' \tag{4}$$

The dependence of the particle flux on the temperature gradient is plotted at ρ=0.3 in Figure 5. Figure 5 shows that for a given temperature gradient the particle flux is lower in the QHS configuration.

7. Neoclassical Calculations

The neoclassical particle and thermal transport were calculated using the DKES code to find the monoenergetic diffusion coefficients [4][5]. At each radial location the monoenergetic diffusion coefficients are numerically integrated over a Maxwellian by using a fit form to the DKES results to yield the neoclassical transport coefficient matrix. The particle and heat fluxes can then be calculated for a given radial electric field. The radial electric field is then determined by the ambipolarity constraint.

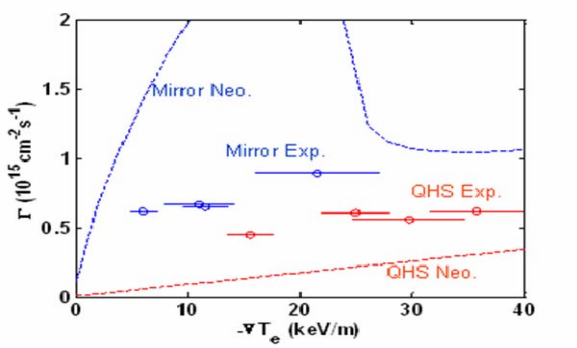

Fig.5 Dependence of the experimental and neoclassical particle flux on temperature gradient.

The neoclassical electron thermal diffusivity profiles for the temperature and density profiles in Figure 2 can be seen in Figure 3. The diffusivity is reduced in the core region due to the strong positive radial electric fields which greatly reduce the ion flux. Figure 3 shows that unlike at B=0.5T, the reduction in the neoclassical transport is not enough to account for the reduction in the experimental transport. This could indicate a reduction in anomalous transport due to quasi-symmetry, however further work on the neoclassical calculations is required as will be explained below.

In Figure 5 the neoclassical calculations also show that for a given temperature gradient the particle flux is expected to be smaller in the QHS configuration. However, the large difference in the neoclassical values is not seen in the experimental results.

As mentioned above, several additional effects and corrections can be applied to the neoclassical calculations, two of which will be briefly described here. The monoenergetic diffusion coefficients calculated by DKES were fit to an analytic form to allow a fast numerical integration over a Maxwellian. The analytic form however did not account for the effect of the poloidal resonance of the radial electric field on the ion flux. To correct for this the analytic form was modified to include this effect. This effect will in the future be more accurately accounted for by performing a very fine DKES scan and directly interpolating the results instead of fitting to an analytic form.

The above method has been applied to many stellarators[6], however DKES only considers pitch angle scattering which results in a collision operator that is not momentum conserving. Due to the symmetric nature of HSX the effect of momentum conservation may be important, as in a tokamak. To address this, the PENTA code [7], which uses a momentum conserving collision operator will be run and compared to the results obtained using DKES and ambipolarity.

8. Conclusion

Initial results at B=1.0T demonstrate a reduction in particle and electron thermal transport due to quasi-symmetry. Profiles from Thomson scattering clearly show an improvement in electron thermal transport, with 2.3 times the injected power required to match the electron temperature profiles. A large (factor of three) reduction in the core electron thermal diffusivity has also been measured. A particle transport analysis indicates that for a given temperature gradient the particle flux is reduced in the QHS configuration. Finally, neoclassical calculations suggest a reduction in anomalous transport in the QHS configuration, but further work is required to confirm this.

References

[1] J.M. Canik *et al*., Phys. Rev. Letters **98**, 085002 (2007).
[2] J.M. Canik, Ph.D. Thesis, University of Wisconsin, Madison, 2007.
[3] D. Heifetz *et al*., J. Comp. Phys. **46**, 309 (1982).
[4] S.P. Hirshman *et al*., Phys. Fluids **29**, 2951 (1986).
[5] W.I. van Rij and S.P. Hirshman, Phys. Fluids B **1**, 563 (1989).
[6] C.D. Beidler *et al*., Proceedings of the 14th ISW, Greifswald, Germany, Sept. 29-Oct. 1, 2003.
[7] D.A. Spong, Phys. Plasmas **12**, 056114 (2005).